Research Article | Vol. 25, No. 8 | 17 Apr 2017 | OPTICS EXPRESS 9368
Optics EXPRESS

Adaptively loaded IM/DD optical OFDM based on set-partitioned QAM formats

JIAN ZHAO[1,*] AND LIAN-KUAN CHEN[2]

[1]*Photonics Systems Group, Tyndall National Institute, Lee Maltings, Dyke Parade, Cork, Ireland*
[2]*Department of Information Engineering, The Chinese University of Hong Kong, Shatin, Hong Kong, China*
[*]*jian.zhao@tyndall.ie*

Abstract: We investigate the constellation design and symbol error rate (SER) of set-partitioned (SP) quadrature amplitude modulation (QAM) formats. Based on the SER analysis, we derive the adaptive bit and power loading algorithm for SP QAM based intensity-modulation direct-detection (IM/DD) orthogonal frequency division multiplexing (OFDM). We experimentally show that the proposed system significantly outperforms the conventional adaptively-loaded IM/DD OFDM and can increase the data rate from 36 Gbit/s to 42 Gbit/s in the presence of severe dispersion-induced spectral nulls after 40-km single-mode fiber. It is also shown that the adaptive algorithm greatly enhances the tolerance to fiber nonlinearity and allows for more power budget.

OCIS codes: (060.2330) Fiber optics communications; (060.4080) Modulation.

References and links

1. Q. Yang, Z. He, Z. Yang, S. Yu, X. Yi, and W. Shieh, "Coherent optical DFT-spread OFDM transmission using orthogonal band multiplexing," Opt. Express **20**(3), 2379–2385 (2012).
2. J. Zhao, "DFT-based offset-QAM OFDM for optical communications," Opt. Express **22**(1), 1114–1126 (2014).
3. P. S. Chow, J. M. Cioffi, and J. A. C. Bingham, "A practical discrete multi-tone transceiver loading algorithm for data transmission over spectrally shaped channels," IEEE Trans. Commun. **43**(2), 773–776 (1995).
4. E. Giacoumidis, A. Kavatzikidis, A. Tsokanos, J. M. Tang, and I. Tomkos, "Adaptive loading algorithms for IMDD optical OFDM PON systems using directly modulated lasers," J. Opt. Commun. Netw. **4**(10), 769–778 (2012).
5. B. Cardiff, M. F. Flanagan, F. Smyth, L. P. Barry, and A. D. Fagan, "On bit and power loading for OFDM over SI-POF," J. Lightwave Technol. **29**(10), 1547–1554 (2011).
6. D. Bykhovsky and S. Arnon, "An experimental comparison of different bit-and-power allocation algorithms for DCO-OFDM," J. Lightwave Technol. **32**(8), 1559–1564 (2014).
7. Z. Yu, H. Chen, M. Chen, S. Yang, and S. Xie, "Bandwidth improvement using adaptive loading scheme in optical direct-detection OFDM," IEEE J. Quantum Electron. **52**(10), 8000106 (2016).
8. M. Karlsson and E. Agrell, "Which is the most power-efficient modulation format in optical links?" Opt. Express **17**(13), 10814–10819 (2009).
9. I. Djordjevic, H. G. Batshon, L. Xu, and T. Wang, "Four-dimensional optical multiband-OFDM for beyond 1.4 Tb/s serial optical transmission," Opt. Express **19**(2), 876–882 (2011).
10. H. Zhang, C. R. Davidson, H. G. Batshon, M. Mazurczyk, M. Bolshtyansky, D. G. Foursa, and A. Pilipetskii, "DP-16QAM based coded modulation transmission in C+L band system at transoceanic distance," in *Technical Digest of Optical Fiber Communication Conference (OFC)* (2016), paper W1I.2.
11. R. R. Muller, J. Renaudier, M. A. Mestre, H. Mardoyan, A. Konczykowska, F. Jorge, B. Duval, and J. Y. Dupuy, "Multi-dimension coded PAM4 signaling for 100Gb/s short reach transceivers," in *Technical Digest of Optical Fiber Communication Conference (OFC)* (2016), Paper Th1G.4.
12. J. Zhao, S. K. Ibrahim, D. Rafique, P. Gunning, and A. D. Ellis, "Symbol synchronization exploiting the symmetric property in optical fast OFDM," IEEE Photonics Technol. Lett. **23**(9), 594–596 (2011).

1. Introduction

Optical orthogonal frequency division multiplexing (OFDM) [1,2] has attracted great interest for optical networks due to high spectral efficiency and efficient channel estimation and equalization. Compared to its coherent counterpart, intensity-modulation and direct-detection (IM/DD) optical OFDM is simple and cost-effective, and is more suitable for cost-sensitive access network and data center connections. Adaptive bit and power loading is an important

#285534 https://doi.org/10.1364/OE.25.009368
Journal © 2017 Received 25 Jan 2017; revised 1 Apr 2017; accepted 11 Apr 2017; published 13 Apr 2017

Optics EXPRESS

technology in IM/DD OFDM [3–7]. By allocating different bits to each individual subcarrier according to the signal to noise ratio (SNR), this technology maximizes the system capacity and increases the flexibility via fine spectral efficiency (SE) granularities.

On the other hand, set-partitioned (SP) quadrature amplitude modulation (QAM) formats, whose constellation points are a subset of a multi-dimensional QAM constellation, have attracted much attention recently in long-haul coherent transmission systems [8–10]. By properly selecting the constellation points, this technology can achieve better power efficiency than the conventional QAM formats at the same data rate. In addition, this technology can generate different SEs with fine granularity without change of hardware, and can balance the performance and SE to meet the requirements of different optical systems. Although this type of formats has been studied in coherent systems, very few works have been done in IM/DD systems. In [11], 4-dimensional coded pulse amplitude modulation (PAM) was proposed in point-to-point short-reach links, enabling high receiver sensitivity, low latency and low complexity. However, to the best of our knowledge, this technology has not been studied in IM/DD OFDM. In particular, conventional adaptive loading algorithm cannot be applied to the SP QAM formats and should be re-designed according to the bound of their symbol error rate (SER).

In this paper, we propose SP QAM based adaptive loading OFDM system. We analyze the constellation design and the SER of different SP QAM formats. We then derive the adaptive bit and power loading algorithm based on the analysis, and demonstrate the technology in a 40-km IM/DD system with data rate varying from 28 Gbit/s to 42 Gbit/s. It is shown that the proposed system exhibits greatly improved performance compared to conventional adaptively-loaded IM/DD OFDM system, and supports >40 Gbit/s data rate after 40-km single-mode fiber (SMF) transmission. The proposed algorithm is also robust to fiber nonlinearity and allows for more power budget.

2. Principle

In this section, we will firstly discuss the constellation design of the SP QAM formats and theoretically analyze their symbol error rates (SER). Then we will use the SER to modify the adaptive bit and power loading algorithm to accommodate the SP QAM formats.

2.1 Constellation design of the SP QAM formats

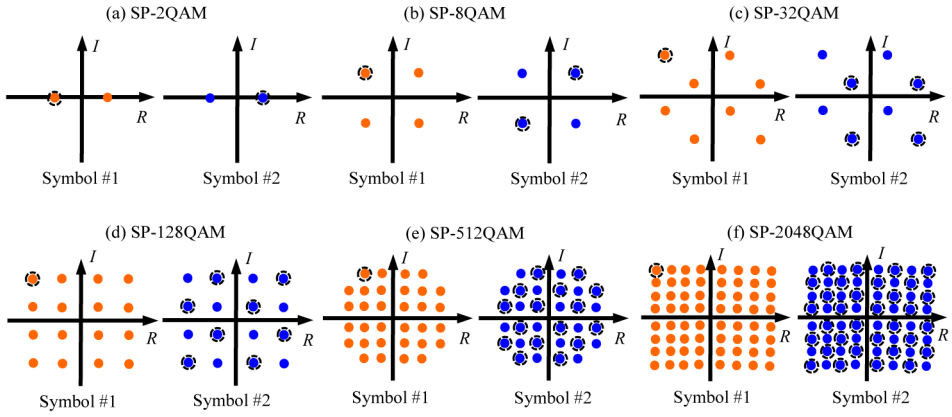

Fig. 1. Constellation of SP-2QAM, SP-8QAM, SP-32QAM, SP-128QAM, SP-512QAM, and SP-2048QAM. In each format, circled points in symbol #2 represent all possible constellation points when the circled point in symbol #1 is selected.

In this paper, every two OFDM symbols of the same subcarrier are jointly encoded to generate SP QAM based OFDM. This principle might be extended to jointly encode two subcarriers within each OFDM symbol. The two consecutive symbols of each subcarrier

Optics EXPRESS

construct a 4-dimensional constellation: the in-phase and quadrature tributaries of symbol #1 and the in-phase and quadrature tributaries of symbol #2 (see Fig. 1). We denote the 4-dimensional constellation, from which a subset of points is selected to construct the SP QAM formats, as super-constellation. The super-constellation is commonly generated by two 2^m conventional QAM constellations (with exception of 8QAM as discussed later), where m is the number of bits carried in the 2-dimensional constellation. As shown in Fig. 1(a), in binary phase shift keying (BPSK), the super-constellation has $2 \times 2 = 4$ points. In SP-2QAM, when the constellation point in symbol #1 is the marked one, (−1, 0), only the point marked in symbol #2 is selected; when the constellation point in symbol #1 is the unmarked one, (1, 0), only the unmarked point in symbol #2 is selected. The number of bits in SP-2QAM is 1 and the Euclidean distance is increased by $2^{1/2}$ compared to conventional BPSK. Similarly, in quadrature phase shift keying (QPSK), the super-constellation has $4 \times 4 = 16$ points. SP-8QAM, also known as polarization switched QPSK in coherent systems, selects 8 points from the super-constellation to increase the Euclidean distance by $2^{1/2}$: when the point in symbol #1 is (−1, 1) or (1, −1), only points of (−1, −1) and (1, 1) are selected in symbol #2; when the point in symbol #1 is (−1, −1) or (1, 1), only points of (−1, 1) and (1, −1) are selected in symbol #2. We can thus generalize one necessary requirement of the 2-dimension QAM constellation that can generate SP QAM formats with increased Euclidean distance by $2^{1/2}$: it can be divided into two subgroups; the minimal Euclidean distance between points within each subgroup is $\geq 2^{1/2}$ times of the minimal Euclidean distance between the points in subgroup #1 and the points in subgroup #2. It is readily proved that conventional optimized 8QAM does not satisfy this requirement. We thus propose the constellation in Fig. 1(c) to construct SP-32QAM. On the other hand, conventional 16QAM, 32QAM, and 64QAM satisfy the condition, and can be used to generate SP-128QAM, SP-512QAM, and SP-2048QAM, respectively (Fig. 1(d)-(f)).

The SEs of the SP QAM formats in Fig. 1 are 0.5, 1.5, 2.5, 3.5, 4.5, and 5.5, respectively. In this paper, we will use these formats for the proposed bit and power loading algorithm. One advantage of these SP formats, although not fully optimized in terms of power efficiency in the 4-dimensional space, is their simplicity in data mapping: m bits can be used to encode the constellation points in symbol #1 in the same way as in conventional QAM, while another m-1 bits are used to encode the points in symbol #2 given the mapping information in symbol #1. From the Shannon limit of a multicarrier system, adaptive allocation of SEs with a finer granularity may improve the transmission rate because the capacity of each subcarrier is a continuous value while the SE of a practically implemented format is a discrete value. Therefore, in this paper, we also investigate a finer SE granularity, which, in addition to the aforementioned SP QAM formats, combines the low (or high) level constellation in symbol #1 and the high (or low) level constellation in symbol #2 to achieve SEs of 1, 2, 3, 4, and 5. For example, the constellation of symbol #1 in SP-128QAM is combined with the constellation of symbol #2 in SP-512QAM to generate the SE of 4. Note however that a finer granularity does not guarantee improved performance because it is also related to the implementation of formats for the finer granularity, including their bit error rate performance, robustness to interference and nonlinearity etc.

2.2 Symbol error rate of the SP QAM formats

In order to derive the adaptive bit and power loading algorithm for the SP QAM formats, we firstly study their SER, aiming to obtain a general SER bound for all these formats. Under additive white Gaussian noise (AWGN), the SER can be generalized as:

$$SER = K \cdot Q\left(\frac{d_{\min}}{\sqrt{2N_0}}\right) \tag{1}$$

Optics EXPRESS

where K is an coefficient used to evaluate the average number of points that have the minimal Euclidean distance to the investigated point in the constellation. d_{min} is the minimal Euclidean distance, and is related to the average power per symbol and the constellation design of signal formats. N_0 is the power spectral density of the noise. Note that although Eq. (1) is derived under AWGN, it can also be used to estimate the SER under other noise and distortions by including their effects in N_0. Based on Eq. (1), it has been well studied in the literature that the SER in conventional 2^m QAM formats, where m is an even number, is:

$$SER \approx 4\times(1-\frac{1}{2^{m/2}})Q(\sqrt{\frac{3}{2^m-1}SNR}) < 4\times Q(\sqrt{\frac{3}{2^m-1}SNR}) \quad (2)$$

where SNR is defined as:

$$SNR = E_s / N_0 \quad (3)$$

In Eq. (3), E_s is the average power per symbol. In practice, SNR can be obtained using channel estimation, as will be discussed later. The SP QAM formats are based on the conventional QAM and increase the Euclidean distance by $2^{1/2}$. Also note that SP QAM formats have 0.5-bit loss of SE per symbol compared to the conventional QAM. We can thus derive the SER, where $m + 1/2$ is an even number, as:

$$SER < K\times Q(\sqrt{\frac{3\times 2}{2^{m+1/2}-1}SNR}) \quad (4)$$

where K should be re-determined in the 4-dimensional constellation. We take a constellation point in SP-128QAM as an example: (−1, 1) in symbol #1 and (1, 1) in symbol #2 (see Fig. 2). We divide the super-constellation into two subgroups, represented by solid and empty circles: when the point in symbol #1 is the solid (or empty) point, only the solid (or empty) points in symbol #2 can be selected. For the fixed point (−1, 1) in symbol #1, there are four empty points in symbol #2 that have the minimal distance of 2 to (1, 1), and another four solid points that have the minimal distance of $2 \times 2^{1/2}$ to (1, 1). Similar result applies to (−1, 1) in symbol #1 when (1, 1) in symbol #2 is fixed. Therefore, for (−1, 1, 1, 1) in SP-128QAM, there are $4 + 4 + 4 \times 4 = 24$ points that give the minimal distance of $2 \times 2^{1/2}$. In this case, K in Eq. (4) is 24/2 = 12. Some points in the constellation may have a smaller K but 12 can be used as an upper bound for K.

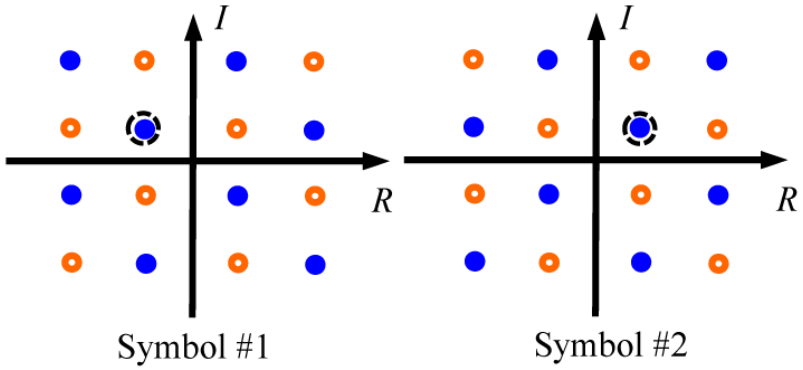

Fig. 2. Constellation of SP-128QAM, which is divided into two subgroups represented by solid and empty circles, respectively. The minimal distance between the 16 points in the constellation of either symbol #1 or symbol #2 is assumed to be 2.

Optics EXPRESS

Table 1. Upper bound of SER for different SP QAM formats

Format	SP-2QAM	SP-8QAM	SP-32QAM	SP-128QAM	SP-512QAM	SP-2048QAM
Equation (1)	$Q(\sqrt{4SNR})$	$3\cdot Q(\sqrt{2SNR})$	$10\cdot Q(\sqrt{\frac{4SNR}{5}})$	$12\cdot Q(\sqrt{\frac{2SNR}{5}})$	$12\cdot Q(\sqrt{\frac{SNR}{5}})$	$12\cdot Q(\sqrt{\frac{2SNR}{21}})$
Equation (4)	$K\cdot Q(\sqrt{6SNR})$	$K\cdot Q(\sqrt{2SNR})$	$K\cdot Q(\sqrt{\frac{6SNR}{7}})$	$K\cdot Q(\sqrt{\frac{2SNR}{5}})$	$K\cdot Q(\sqrt{\frac{6SNR}{31}})$	$K\cdot Q(\sqrt{\frac{2SNR}{21}})$

From Eq. (4), the key differences of SER for the SP QAM formats, compared to the conventional QAM, are the increased Euclidean distance by $2^{1/2}$, the loss of the SE by 0.5 bit, and the coefficient of K to evaluate the average number of points giving the minimal distance. Although Eq. (4) is only precise when m + 1/2 is even, it is still a good approximation for the SER when m + 1/2 is odd. By using the general SER equation (Eq. (1)), we can get the SER performance of different SP QAM formats, as shown in Table 1. The approximation using Eq. (4) is also given in the table, where K is upper bounded by 12.

Finally, as mentioned in Section 2.1, we may combine the low (or high) level constellation in symbol #1 and the high (or low) level constellation in symbol #2 to achieve SEs of 1, 2, 3, 4, and 5. In these cases, the power to achieve a certain SER is the average of the low-level and high-level constellations, and so the SER can still be estimated by Eq. (4).

2.3 Adaptive bit and power loading algorithm for the SP QAM formats

From Section 2.2, we have shown that the SER of the SP QAM formats shown in Fig. 1 can be estimated by Eq. (4). This SER is different from that of conventional QAM. As a result, conventional adaptive algorithm [3] cannot be applied to the SP QAM formats. In particular, the equations for bit allocation should be re-derived based on the SER in Eq. (4). In SP QAM based OFDM, if the SNR of the i^{th} subcarrier, SNR_i, is obtained, we can derive the number of bits in that subcarrier by re-writing Eq. (4) as:

$$m_i = \log_2(1+\frac{3\times 2\times SNR_i}{(Q^{-1}(SER_{pre-set}/K))^2}) - 0.5 \tag{5}$$

$$\hat{m}_i = round(m_i + 1/2) - 1/2 \tag{6}$$

where $SER_{pre\text{-}set}$ is the pre-set SER. $SER_{pre\text{-}set}$ may not match that in the real system, and so by referring to the Chow's algorithm [3], we revise Eq. (5) as:

$$m_i = \log_2(1+\frac{3\times 2\times SNR_i}{(Q^{-1}(SER_{pre-set}/K))^2\cdot\gamma}) - 0.5 \tag{7}$$

where γ is a parameter to be determined by iteration. The convergence of bit allocation is similar to that in [3]. Note that when a finer SE granularity is used, the subtracted/added bit at each time during the convergence of bit allocation is 0.5 bit instead of 1 bit. After the bit allocation, the power of each subcarrier is adjusted by using the SER of Eq. (1) in Table 1.

The calculation of Eq. (7) depends on the estimation of SNR_i for each subcarrier. In practice, it is desired that SNR_i includes not only noise but also the effect of signal distortions. This would enable the adaptive algorithm robust to impairments such as interference and fiber nonlinearity. In this paper, SNR_i is estimated by calculating the correlation between the received signal and the transmitted signal:

Optics EXPRESS

$$SNR_i = \frac{\left|E(r_i^* \cdot s_i)\right|^2}{E(|r_i|^2)E(|s_i|^2) - \left|E(r_i^* \cdot s_i)\right|} \tag{8}$$

where r_i and s_i are the received and transmitted signal in the i^{th} subcarrier. In order to realize Eq. (8), a training sequence is required for estimation of the SNR_i before the payload is sent.

The proposed algorithm, compared to the conventional QAM algorithm [3], only modifies the allocation equations (Eqs. (5)-(7)) and does not introduce additional complexity. Also note that although the decoding of SP QAM formats in the 4-dimensioinal space is more complicated than that of conventional QAM, there are methods to reduce this decoding complexity, and the overall complexity of SP QAM based OFDM including modules such as (de-)multiplexing, equalization etc. is still comparable to that of the conventional OFDM.

3. Experimental setup and results

3.1 Experimental setup

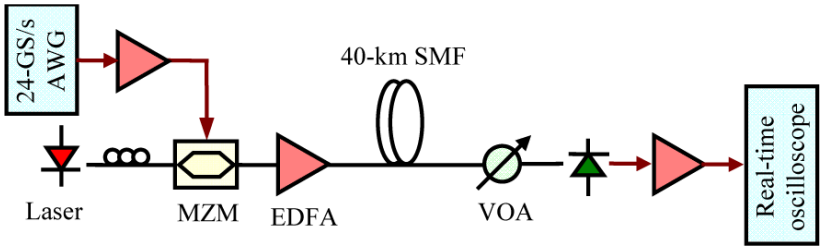

Fig. 3. Experimental setup.

Figure 3 shows the experimental setup. The OFDM signal consisted of 63 subcarriers and the point size of the fast Fourier transform (FFT) was 128. The first subcarrier was zero-padded, allowing for AC-coupled amplifiers. For adaptive bit and power loading, 8QAM OFDM signal was firstly used to estimate the SNR via Eq. (8) and the number of bits was then calculated based on Eq. (7). The length of cyclic prefix was 4 and the peak to average power ratio was set to be 11 dB by clipping. The OFDM signal was uploaded into a 24-GS/s arbitrary waveform generator (AWG) with ~7-GHz analogue bandwidth (without sinc roll-off). Pre-equalization was included to compensate the limited bandwidth of the AWG and the sinc roll-off in D/A conversion. The data rate (including the cyclic prefix) varied from 28.3 Gbit/s to 42.5 Gbit/s. A laser with ~5-MHz laser linewidth was used to generate the CW light. A Mach-Zehnder modulator (MZM) was used for modulation and the input electrical peak-to-peak voltage was ~$V_\pi/2$. The optical signal was amplified by an Erbium doped fibre amplifier (EDFA) and transmitted over 40-km SMF. At the receiver, the optical signal was detected by a photodiode. A variable optical attenuator (VOA) was used to vary the received power. The detected signal was electrically amplified and sampled by a 50-GS/s real-time oscilloscope. The start-of-frame symbol was firstly detected for symbol synchronization [12]. The signal was equalized using one-tap equalizer. The Euclidean distances between the equalized signal and the means of all possible transmitted constellation points were calculated, and the minimal distance was found to decode the signal. ~1M bits were measured and bit error rate (BER) was obtained by direct error counting.

Optics EXPRESS

3.2 Experimental results

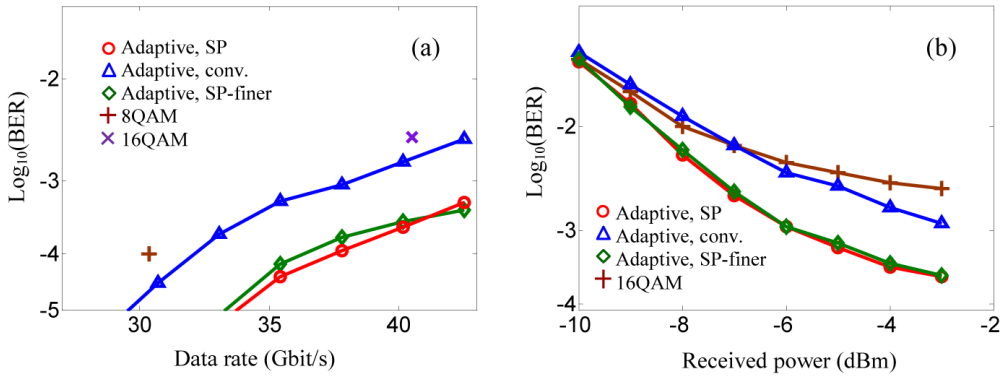

Fig. 4. (a) BER performance versus signal data rate at back-to-back when the signal formats are 8QAM, 16QAM, adaptively-loaded conventional QAM, adaptively-loaded SP QAM, and SP QAM with the finer SE granularity. The received signal power is −3 dBm. (b) BER versus the received power for different formats when the data rate is 40.2 Gbit/s.

We firstly investigate the back-to-back performance of the proposed algorithm. Figure 4(a) shows the BER versus the signal data rate using different bit and power loading algorithms. The SNR is estimated when the received power is −3 dBm. The performances of 8QAM and 16QAM are also shown for comparison. When a single format is used, 54 out of 64 data subcarriers are modulated so that the data rates are ~30 Gbit/s and 40 Gbit/s for 8QAM and 16QAM, respectively. From the figure, it is seen that at the same data rate, conventional loading algorithm can get slight performance improvement compared to systems with a single format for all subcarriers. Adaptive loading of the SP QAM formats significantly improves the performance, with around one order of magnitude reduction in BER. It is also shown that loading of SP QAM formats with the finer SE granularity (SE = 0.5, 1, 1.5… 5.5) exhibits similar performance as that by employing the coarse SE granularity (SE = 0.5, 1.5 … 5.5). This might be because the difference of these two SE granularities is small and the formats for SE of 1, 2, 3, 4, and 5 show higher sensitivity to nonlinear distortions due to non-uniform power of adjacent symbols (please refer to the design of these formats in subsection 2.1). Therefore, in our investigation, the coarse granularity is sufficient to balance the performance and complexity. Figure 4(b) shows BER versus received power at the receiver. The SNR is estimated when the received power is −3 dBm. At the back-to-back, the channel is flat without spectral nulls. Therefore, the performance of conventional loading algorithm is similar to that using a single format. The proposed scheme outperforms the conventional loading algorithm due to enhanced Euclidean distance. At the received power of −3 dBm, the BERs of the conventional and proposed algorithms are 10^{-3} and 2.5×10^{-4}, respectively.

Next, we study the transmission performance of the proposed algorithm. Figure 5(a) shows the BER versus the signal data rate after 40-km SMF. Figure 5(b) depicts the allocated SE over subcarriers at 40.2 Gbit/s, as well as the measured SNR profiles. In (a) and (b), the SNR is estimated when the received power is −3 dBm and the signal launch power is 10 dBm. It is clearly seen that there is a spectral null (see Fig. 5(b)), induced by the joint effect of dispersion and the square-law direct detection. The position of nulls, f_{null}, can be estimated by $\cos(\beta_2 L/2 \times (2\pi f_{\text{null}})^2) = 0$ and is calculated as ~10 GHz, where β_2 is the dispersion parameter and L is the fiber length. From Fig. 5(a), it is seen that there is significant performance degradation when a single format is employed for all subcarriers, and the achievable BERs of both 30-Gbit/s 8QAM and 40-Gbit/s 16QAM are above 10^{-2}. By using conventional loading algorithm, formats are allocated according to the estimated SNR and low-level formats are assigned around the spectral null, resulting in improved performance. However, at the BER of

Optics EXPRESS

3.8 × 10^{-3}, the supported data rate is still limited to ~36 Gbit/s. By using the proposed algorithm, significant performance improvement is observed and ~42-Gbit/s data rate can be supported at 40 km.

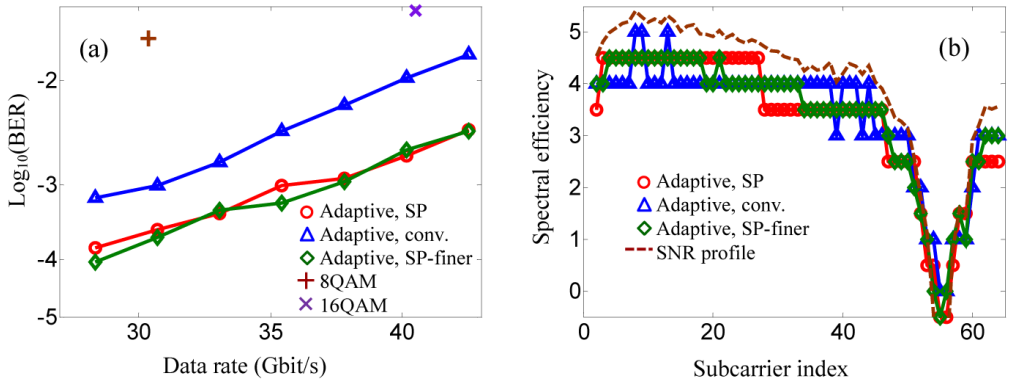

Fig. 5. (a) BER performance versus signal data rate after 40 km when the signal formats are 8QAM, 16QAM, adaptively-loaded conventional QAM, adaptively-loaded SP QAM, and SP QAM with the finer SE granularity. (b) SE versus subcarrier index for adaptively-loaded conventional QAM, SP QAM, and SP QAM with the finer SE granularity at 40.2 Gbit/s. The dashed line represents the estimated SNR profile (= SNR (dB) /3). In (a) and (b), the received signal power is −3 dBm and the signal launch power into the fiber is 10 dBm.

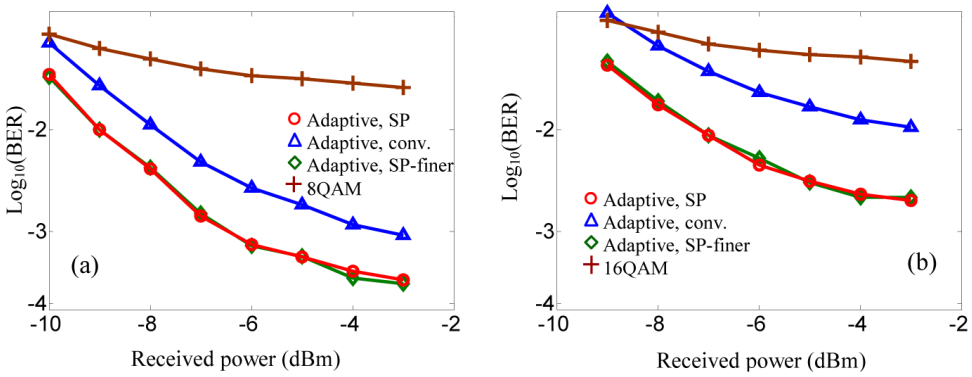

Fig. 6. BER versus received power after 40 km when the data rate is (a) 30.7 Gbit/s and (b) 40.2 Gbit/s. The signal launch power is 10 dBm and the MZM bias is 2.4 V.

Figure 6 depicts the BER of different formats when the data rate is (a) 30.7 Gbit/s and (b) 40.2 Gbit/s. The SNRs are estimated when the received power is −3 dBm and the signal launch power is 10 dBm. In contrast to Fig. 4(b), conventional adaptive algorithm exhibits much better performance than that using a single format for all subcarriers when there is a dispersion-induced spectral null. At the received power of −3 dBm, the BERs of the conventional loading algorithm are 1 × 10^{-3} and 1 × 10^{-2} in (a) and (b), respectively. When the proposed algorithm is employed, the BER is reduced below 3.8 × 10^{-3} at 40 Gbit/s. Similar to the back-to-back case, the finer granularity does not show further performance improvement. In the following studies, the coarse granularity is used in the proposed algorithm.

Optics EXPRESS

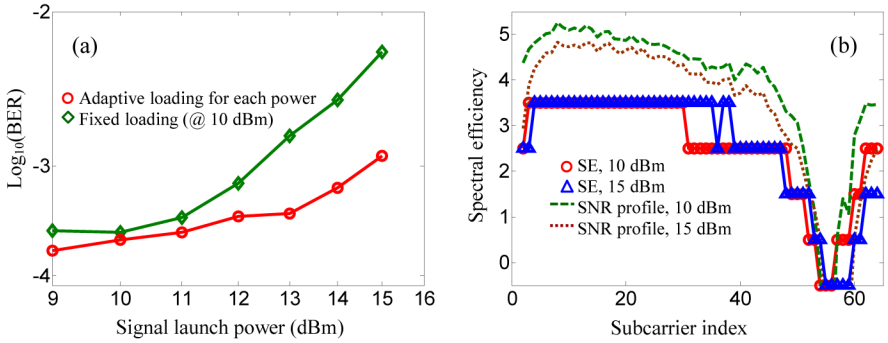

Fig. 7. (a) BER versus the launch power into the 40-km SMF when channel estimation and bit loading are performed for each power (circles) or are fixed using the SNR profile obtained at 10-dBm launch power (diamonds). (b) SE versus subcarrier index when the bits are loaded using the SNR profiles estimated at 10-dBm and 15-dBm launch power. Dashed and dotted lines represent the SNR profiles (= SNR (dB) / 3). In (a) and (b), the data rate is 30.7 Gbit/s.

The proposed adaptive loading algorithm can enhance the tolerance to fiber nonlinearity. Figure 7(a) depicts the BER versus signal launch power into the fiber when the algorithm estimates the SNR for each signal launch power (circles) or uses a fixed SNR profile obtained at the launch power of 10 dBm (diamonds). It is seen that fiber nonlinear effect is negligible for 10-dBm launch power (as used in Figs. 4-6) and becomes prominent when the power increases beyond 12 dBm. Estimation of the SNR profile for each power increases the complexity but significantly improves the performance. Figure 7(b) depicts the loaded SE levels over subcarriers and the estimated SNR profiles for powers of 10 dBm and 15 dBm. The SNR estimation in Eq. (8) includes not only AWGN but also nonlinear noise. Therefore, it is seen from Fig. 7(b) that the SNR decreases as the launch power increases. When the algorithm re-allocates the SEs according to the estimated SNR profile for each power, significant performance improvement can be obtained. At the launch power of 15 dBm, the BER can be reduced from 6×10^{-3} to 1.2×10^{-3} at 30.7 Gbit/s (see Fig. 7(a)).

Finally, we investigate the performance sensitivity to the modulator bias. In the experiment, the optimal bias might drift over time with the range of ~0.2 V due to the temperature variation. Figure 8(a) shows the BER versus the bias when the algorithm estimates the SNR profile for each bias or uses the fixed SNR measured under 2.4-V bias. Figure 8(b) depicts the allocated SEs over subcarriers and the measured SNR profiles. It is seen that the system shows similar performance when the bias changes from 2 V to 2.5 V, which is sufficiently wide to tolerate the bias drifting in the experiment. In addition, the difference of the SNR profiles for the bias of 1.8 V and 3 V is not significant, implying that the SNR does not have to be estimated each time to avoid the complexity.

Optics EXPRESS

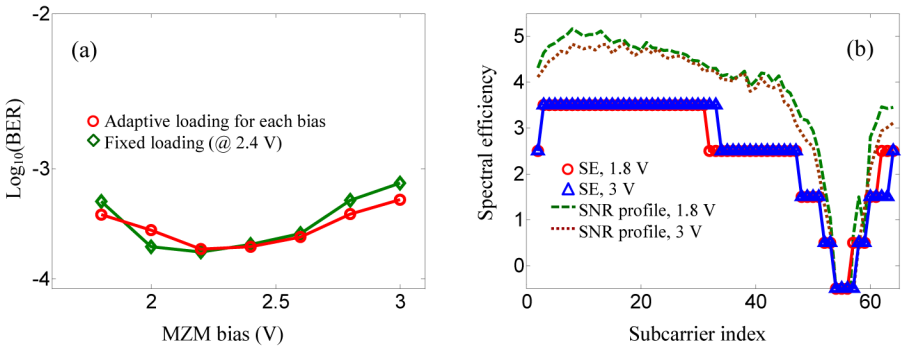

Fig. 8. (a) BER versus the MZM bias when the channel estimation and bit loading are performed for each bias (circles) or are fixed using the SNR profile obtained at 2.4-V bias (diamonds). (b) SE versus subcarrier index when the bits are loaded using the SNR profiles estimated at 1.8-V and 3-V bias. Dashed and dotted lines represent the SNR profiles (= SNR (dB) / 3). In (a) and (b), the signal data rate is 30.7 Gbit/s.

4. Summary

We have derived an adaptive loading algorithm for SP QAM based IM/DD OFDM, and experimentally shown that the proposed system significantly outperforms the conventional adaptively-loaded IM/DD OFDM. We have demonstrated > 40 Gbit/s over 40-km SMF using this technology. It is also shown that the proposed algorithm, by including the nonlinear noise in the SNR estimation and bit/power loading, greatly enhances the tolerance to fiber nonlinearity and enables more power budget. The proposed technology is potential to alleviate the challenges of IM/DD systems for higher data rate and longer transmission reach while maintaining low cost and complexity.

Funding

Science Foundation Ireland (SFI) grants 15/CDA/3652 and 11/SIRG/I2124, and HK SAR RGC grants GRF14200914 and GRF14204015.